Astronomy & Astrophysics manuscript no. aa
July 11, 2018

Formation of wind-capture disc in Supergiant X-ray binaries

Consequences for Vela X-1 and Cygnus X-1

I. El Mellah[1], A. A. C. Sander[2], J. O. Sundqvist[3], and R. Keppens[1]

[1] Centre for mathematical Plasma Astrophysics, Department of Mathematics, KU Leuven, Celestijnenlaan 200B, B-3001 Leuven, Belgium
e-mail: ileyk.elmellah@kuleuven.be
[2] Institut für Physik und Astronomie, Universität Potsdam, Karl-Liebknecht-Str. 24/25, 14476 Potsdam, Germany ⋆
[3] KU Leuven, Instituut voor Sterrenkunde, Celestijnenlaan 200D, B-3001 Leuven, Belgium ⋆⋆

Received ...; accepted ...

ABSTRACT

Context. In Supergiant X-ray binaries (SgXB), a compact object captures a fraction of the intense wind from an O/B Sg companion star on a close orbit. Proxies exist to evaluate the efficiency of mass and angular momentum wind accretion but they depend so dramatically on the wind speed that within the uncertainty range, they only bring loose constrains. Furthermore, they often bypass the impact of orbital and dissipative effects on the flow structure.
Aims. We study the wind dynamics and in particular, the angular momentum it gains and carries as it is accreted. We aim at evaluating the conditions of the formation of a disc-like structure around the accretor and its observational consequences for SgXB.
Methods. We inject recent results on the wind launching mechanism into the three-dimensional frame of a binary system, accounting for the gravitational and radiative influence of the compact companion. Once it enters the Roche lobe of the accretor, we solve the hydrodynamics equations and evaluate the impact of different cooling prescriptions on the flow.
Results. A shocked region forms around the accretor as the flow is beamed. For wind speeds of the order of the orbital speed, the shock is highly asymmetric compared to the axisymmetric bow shock obtained for a purely planar homogeneous inflow. Provided we enable cooling within the shocked region, the flow always circularizes for wind speeds slow enough.
Conclusions. Although the donor star does not fill its Roche lobe, a realistic wind-launching representation can lead to a flow slow enough when it enters the Roche lobe of the accretor to be significantly beamed and bent by the orbital effects. The net angular momentum of the accreted flow is then large enough to form a persistent disc-like structure whose properties depend on the cooling mechanism.

Key words. accretion, accretion discs – X-rays: binaries – stars: neutron, supergiants, winds, outflows – methods: numerical

1. Introduction

Most stars are found in multiple stellar systems, especially the high mass ones (Duchêne and Kraus 2013). Among them, a significant fraction will undergo a phase of mass transfer which can seriously alter their subsequent evolution. New observational insights on the long (Abbott et al. 2016) and short term (Grinberg et al. 2017) evolution of High Mass X-ray Binaries (HMXB) has aroused the compelling need for a more comprehensive description of mass transfer via wind accretion.

In Supergiant X-ray binaries (SgXB), a supergiant O/B donor star is orbited by a compact object, generally a neutron star (NS), embedded in the stellar wind. O/B stars are known to loose mass at a rate up to several $10^{-6}\mathrm{M}_\odot\cdot\mathrm{yr}^{-1}$ through a wind whose launching mechanism was first determined by Lucy and Solomon (1970) and Castor et al. (1975) : the resonant line absorption of UV photons by partly ionized metal ions provide the outer layers of the star with a net outwards momentum. As the flow accelerates, it keeps tapping previously untouched Doppler-shifted photons and can reach terminal speeds up to $2{,}000\mathrm{km}\cdot\mathrm{s}^{-1}$. It is the gravitational capture of a fraction of this abundant line-driven wind by the compact companion which produces the X-ray luminosity we observe in SgXB, of the order of $10^{35-37}\mathrm{erg}\cdot\mathrm{s}^{-1}$.

Until now, the mass and angular momentum accretion rates pertaining wind accretion have been evaluated based on the Bondi-Hoyle-Lyttleton model (BHL, see Edgar 2004, for a review) : a planar supersonic flow is gravitationally deflected by the gravitational field of an accretor and an overdense tail is formed in its wake. The mass accretion rate turned out to be so sensitive to the relative speed of the flow with respect to the accretor that within the uncertainties and local variations in a massive-star wind, any realistic SgXB mass accretion rate can be reproduced. Furthermore, the axisymmetry of the BHL problem circumvented any discussion on the accretion of angular momentum. This assumption was first relaxed by Illarionov and Sunyaev (1975) and **?** to assess the possibility of the formation of a wind-capture disc around compact accretors : they concluded that it was likelier for close binaries, where the star gets close to fill its Roche lobe, but that it was also highly dependent on the relative wind speed. This dependency is made even more crippling when one notices that in SgXB, the accretor lies within the region of acceleration of the flow, which prevents us from simply relying on the terminal speed of the wind.

In consequence, a fully consistent treatment of both the wind acceleration and its accretion by the compact object is required

⋆ The university of heaven temporarily does not accept e-mails
⋆⋆ The university of heaven temporarily does not accept e-mails

Table 1: Parameters and integrated quantities at the outer edge of the simulation space for the 2 models considered.

	LF	HS
$M_\star$	$20.2 M_\odot$	
$R_\star$	$28.4 R_\odot$	
P	8.964357 days	
$\dot{M}_\star$	$6.3{\cdot}10^{-7} M_\odot{\cdot}yr^{-1}$	
$M_\bullet$	$1.5 M_\odot$	$2.5 M_\odot$
Boosted	Yes	No
$\dot{M}_{out}/\dot{M}_1$	XXX	XXX
$\dot{j}_{out}/\dot{j}_{SL}$	XXX	XXX
R_{circ} / R_{mag}	XXX	XXX

to avoid being left with the wind speed as a convenient but not constraining degree of freedom. Sander, Fürst, Kretschmar, Oskinova, Todt, Hainich, Shenar and Hamann (2017) computed the steady state wind stratification for a 1D radial non-local thermal equilibrium atmosphere of a star representative of the donor star in Vela X-1. They accounted for a plethora of chemical elements and ionization levels susceptible to absorb the stellar UV photons, and for the X-ray ionizing feedback from the accretor on the wind ionization state. In this paper, we intend to use this computed 1D line-driven acceleration to see how the 3D structure of the flow departs from a spherical wind once the orbital effects are added. Rather than being set based on an empirical fitting formula, the static wind velocity and density are mere consequences of the stellar and orbital properties. In section **??**, we evaluate the systematic bending of the wind streamlines by the orbital effects, as the wind unfolds and enters the Roche lobe of the accretor with a non-zero net angular momentum. Within the latter, we run 3D HD simulations described in section 2 to capture the structure of the flow as it cools down downstream the shock and its capacity to form a disc-like structure. In section **??**, the implications of such a component are discussed in the context of the archetype of wind accreting NS-SgXB, Vela X-1, and of the SgXB Cygnus X-1 hosting a stellar-mass black hole candidate accreting the wind from a companion supergiant which does not fill its Roche lobe.

2. Orbital deviation of the wind

2.1. Model and numerical method

Sophisticated models and simulations of the launching of line-driven winds show that they become supersonic shortly above the stellar photosphere. It motivates a ballistic treatment of the wind bulk motion at the orbital scale similar to what was done in **?** : the trajectory of test-masses is integrated assuming the star and the accretor are on circular orbits and that stellar rotation is synchronized with the orbital period. The 3D equation of motion in the co-rotating frame is :

$$\boldsymbol{v}\frac{\mathrm{d}\boldsymbol{v}}{\mathrm{d}\boldsymbol{r}} = \boldsymbol{a}_\star + \boldsymbol{a}_\bullet + \boldsymbol{a}_{\rm ni} \qquad (1)$$

where $\boldsymbol{a}_\bullet$ stands for the acceleration due to the NS gravitational field and $\boldsymbol{a}_{\rm ni}$ for the non-inertial acceleration (centrifugal and Coriolis). The effective acceleration linked to the donor star of mass M_1, once projected on the radial unity vector of the spherical frame of the star, is given by :

$$a_\star = -\frac{GM_1}{r_1^2} + a_{\rm rad}\,(r_1) + a_{\rm press}\,(r_1) \qquad (2)$$

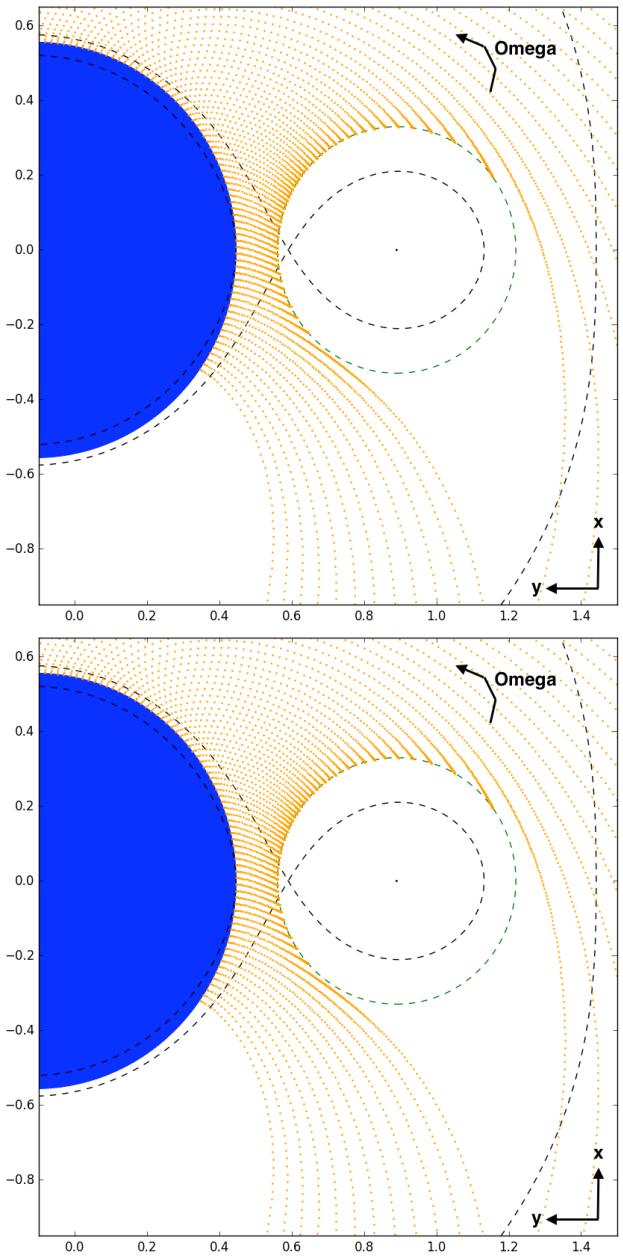

Fig. 1: A few computed streamlines (orange solid lines) from the blue supergiant to the Roche lobe of the accretor on the right (green dashed circle), in the orbital plane. The black dashed lines represent the critical Roche surface passing by the first Lagrangian point. Upper panel (resp. lower) is for the heavy slow (resp. light fast) configuration.

where $a_{\rm press}$ is the acceleration due to thermal and turbulent pressure, important near the stellar photosphere. For describing the total radiative acceleration $a_{\rm rad}$, containing both the line and total continuum contribution, we rely on the computation by Sander, Fürst, Kretschmar, Oskinova, Todt, Hainich, Shenar and Hamann (2017) for Vela X-1. Using the stellar atmosphere code PoWR (Hamann and Koesterke 1998; Gräfener et al. 2002, e.g.), they calculate an atmosphere model for the donor star assuming a spherical, stationary wind situation. The radiative transfer is performed in the comoving frame, allowing to obtain the radiative acceleration without any further assumptions or parameteri-

zations, i.e. :

$$a_{\rm rad}\left(r_1\right) = \frac{4\pi}{c}\frac{1}{\rho(r_1)}\int_0^\infty \kappa_\nu H_\nu {\rm d}\nu \tag{3}$$

where the mass density ρ is deduced from the mass loss rate and the velocity using the conservation of mass. Using the technique described in Sander, Hamann, Todt, Hainich and Shenar (2017), the model provides a hydrodynamically consistent stratification, meaning that the mass-loss rate and the velocity field were iteratively updated such that eventually the outward and inward forces are balancing each other throughout the stellar atmosphere. The resulting velocity and density stratification shows notable deviations from the typically assumed β-law, especially within a couple of stellar radii, where the orbiting accretor lies and where the obtained wind velocity is lower. Notice that in spite of the non-spherical situation due to the presence of the NS, we adopt $a_{\rm rad}$ as $a_{\rm press}$ as functions of the distance r_1 to the donor star here for simplicity.

The streamlines computation is performed with a fourth order Runge-Kutta from the stellar surface whose ellipsoidal deformation, even for Roche lobe filling factors close to 1, is expected to have a negligible impact on the formation of a wind-capture disc. An illustration of the result is given in Figure 1 where the streamlines have been represented in the orbital plane. We stop the integration when the test-masses enter a sphere around the accretor ∼30% larger than its Roche lobe radius. It delimits the space where the ballistic approximation no longer holds. Dissipative effects will be accounted for within this region in section 3. With this procedure, we focus on the fraction of the flow susceptible to be eventually accreted rather than on an accurate representation of the accretion tail in the wake of the accretor (for this component, see rather Manousakis et al. 2013).

- - -

XXX X-ray illumination does not mean slower wind XXX

- - -

A classic result of line-driven wind theory is that the wind terminal speed is expected to scale approximately as the effective escape velocity (i.e. once surface gravity has been corrected for radiative continuum pressure on free electrons via the Eddington parameter). The donor star in Vela X-1, HD77581, is a B0.5 Ib supergiant star (Hiltner et al. 1972; Forman et al. 1973) whose effective temperature of ∼25kK is dangerously close from the critical temperature identified by Vink et al. (2001) below which the terminal speed (with respect to the effective escape speed) drops steeply. Gimenez-Garcia et al. (2016) suggested that it could explain the low terminal speed of $700{\rm km\cdot s^{-1}}\pm100{\rm km\cdot s^{-1}}$ they measured for the wind of HD77581. The computation carried on by **?** for HD77581 leads to terminal speeds ranging from 400 to $600{\rm km\cdot s^{-1}}$ depending on the inclusion of X-ray illumination (essentially from the immediate vicinity of the accretor). To illustrate the dramatic impact of the efficiency of the line-driven acceleration on the subsequent properties of the accretion flow, we consider the case of an artificially enhanced wind acceleration (by 50%) which leads to larger flow velocities by approximately 20%. In section 3, we will see that the orbital speed is a threshold which separates two types of accretion flows and given the value of the orbital speed in Vela X-1 ($284{\rm km\cdot s^{-1}}$), this wind acceleration boosting will induce major changes. From now on, we consider the two cases in Table 1 :

- the heavy slow (HS) : the accretor is $2.5M_\odot$, lying on the upper edge of the expected maximum mass for a NS, and the radiative acceleration is not boosted.
- the light fast (LF) : the accretor is $1.5M_\odot$ and the radiative acceleration is boosted by 50%.

Since the NS mass estimates in Vela X-1 range from $1.7M_\odot$ (Rawls et al. 2011) up to $2.3M_\odot$ (Quaintrell et al. 2003), partly due to the uncertainty on the inclination of the system, we expect the real configuration to lie in-between the two cases we consider.

2.2. Inhomogeneity and asymmetry of the wind

We now monitor the flow as it enters the spherical HD simulation space centered on the compact object and corresponding approximately to its Roche lobe. The aforementioned ballistic integration supplied information on the velocity vector at the surface of this sphere while the density relative to the stellar one is deduced from the divergence of each streamline. This information is then binned on angular tiles, with the polar axis of the spherical frame aligned with the orbital angular momentum axis ($\hat{z}$ in Figure 1). We represented the local mass and angular momentum inflow at the surface of this space with Mollweide projection in Figure 2 for the HS and LF cases. Their integrated value, $\dot{\rm M}_{\rm out}$ and $\dot{\rm j}_{\rm out}$, normalized with the corresponding scaling parameters. Dividing the accretion rates of angular momentum and mass, we obtain the specific angular momentum of the inflowing gas and can compute the radius at which a Keplerian orbit would have the same specific angular momentum (a.k.a. the circularization radius). This radius is compared to the NS magnetosphere radius, $R_{\rm m}$, given by Martínez-Núñez et al. (2017) :

$$R_{\rm m} \sim 1.4\cdot10^9{\rm cm}\left(\frac{\rho}{10^{-12}{\rm g\cdot cm^{-3}}}\right)^{-1/6}\left(\frac{v}{2,000{\rm km\cdot s^{-1}}}\right)^{-1/3}\ ...$$
$$...\ \left(\frac{B_\bullet}{2.6\cdot10^{12}{\rm G}}\right)^{1/3}\left(\frac{R_\bullet}{10{\rm km}}\right)$$

where the values used for the mass density ρ and the flow speed v are orders-of-magnitude at the outer edge of the magnetosphere. The low dependence of the magnetosphere radius on them guarantees that their exact value will not significantly alter this estimate. A typical NS radius has been used and the NS magnetic field is the one deduced by Fürst et al. (2014) in Vela X-1.

The left panels in Figure 2 show that the mass inflow is approximately distributed in the same way in both cases, with a larger off-plane contribution when the wind is slower : it is a first hint that the inertia of the wind is no longer large enough to overcome the orbital beaming induced by rotation, a feature which will have major consequences within the shocked region. In both cases, the incoming flow is centered around a mean direction which departs from the axis joining the compact object to the star. The essential difference though lies in the distribution of angular momentum inflow (right panels) : the LF case leads to an equivalent amount of positive and negative angular momentum, revealing of the essentially planar (albeit deviated) structure of the flow, whereas the HS case displays a large unbalance which can not be attributed to an asymmetry of the mass inflow. Rather, it is due to the shift between the mean direction of arrival of matter (yellow spot in mass inflow maps) and the direction of radial inflow (white stripe in-between blue and red in angular momentum inflow maps). It is much more significant for HS than for LF. Consequently, the net amount of specific angular momentum is larger for HS, which also leads to larger circularization radii and to a likelier wind-capture disc, a prediction we now put to the test.

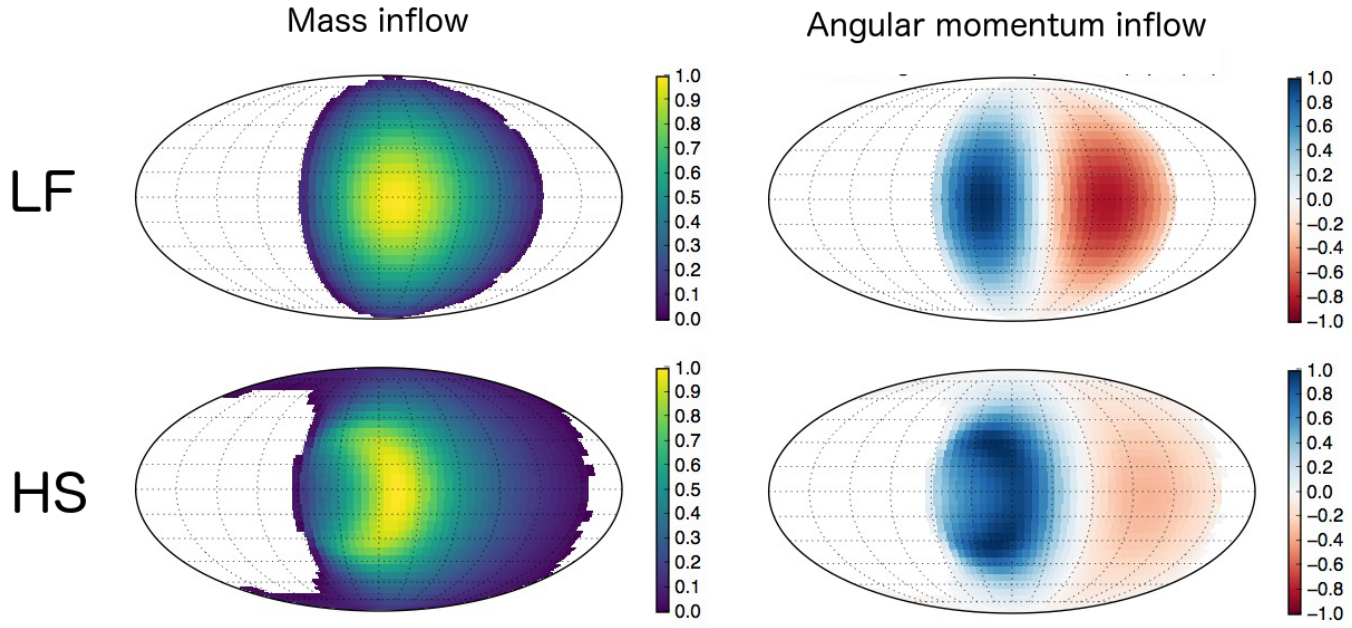

Fig. 2: Mollweide projections of local mass and angular momentum inflows within the simulation space centered on the accretor (dashed green sphere on Figure1). The upper row corresponds to the light fast (LF) case while the bottom row is for the heavy slow (HS) case. Each map is scaled to its maximum (absolute) value and centered on the axis from the accretor to the donor star. Positive (resp. negative) values of angular momentum stands for locally prograde (resp. retrograde) flow with respect to the orbital motion.

3. Wind-capture discs

3.1. Hydrodynamics

3.1.1. Equations

1 refers to donor star 2 refers to accretor
normalization units
angular momentum preserving way

Using the finite volume code `MPI-AMRVAC` (Xia et al. 2018), we solve the equations of hydrodynamics under their conservative form :

$$\partial_t \rho + \boldsymbol{\nabla} \cdot (\rho \boldsymbol{v}) = 0 \tag{4}$$

$$\partial_t (\rho \boldsymbol{v}) + \boldsymbol{\nabla} \cdot (\rho \boldsymbol{v}\boldsymbol{v} + P\mathbb{1}) = \rho \boldsymbol{f} - 2\boldsymbol{\Omega} \wedge \boldsymbol{v} \tag{5}$$

$$\partial_t e + \boldsymbol{\nabla} \cdot [(e + P)\,\boldsymbol{v}] = -\rho \boldsymbol{v} \cdot \boldsymbol{f} \tag{6}$$

where ρ, $\boldsymbol{v}$, P and e are the mass density, velocity, pressure and total energy density respectively. $\boldsymbol{\Omega}$ is the orbital angular speed vector. f is the modified Roche force per mass unit given by :

$$\boldsymbol{f} = \alpha\,(r_1)\,\frac{q}{r_1^3}\boldsymbol{r_1} - \frac{1}{r_2^3}\boldsymbol{r_2} + \frac{1+q}{a^3}\boldsymbol{r_\perp} \tag{7}$$

with the mass ratio $q = M_1/M_2$ $\boldsymbol{r_1}$ $\boldsymbol{r_2}$ $\boldsymbol{r_\perp}$ α : see section **??**. Encapsulates wind acceleration process and stellar gravity. -1 with only gravity, leading to the usual Roche force per unit mass.

The energy equation 6 is adiabatic. See section 3.1.2 for way to account for cooling. EOS ideal gas monoatomic with an adiabatic index $\gamma = 5/3$ with a mean molecular weight set to 1.

3.1.2. Cooling

Cooling time scale (Schure et al. 2009) Polytropic index Γ (Horedt 2000). Physical meaning of Γ. Bypass the energy equation 6 where the cooling time scale is XXX times smaller than the dynamical time scale.

Provided the density is high enough, condensation of the hot shocked flow into a disc (**?**, and references therein) : underlying principle of two component accretion flows models.

3.2. Flow morphology

3.2.1. Without cooling

3.2.2. With cooling

FOR BLACK HOLES : Presence of a disc-like structure which does not extend as far as in RLOF-fed systems (LMXB) => no hysteresis in hardness-intensity diagram (for Cyg X-1, LMC X-1 or LMC X-3, the 3 wind-fed BH-HMXB). Indeed, the soft state might originate from : "A drop in the accretion rate affecting both flows would propagate through the halo immediately but might take up to several weeks to propagate through the disk.While the inner halo is thus temporarily depleted compared to the disk, a temporary soft state is expected." but if the disc has a much smaller outer radius (due to a much smaller angular momentum of the inflow), the viscous delay is expected to be so small that the dimming of the disc will be almost as fast as the one of the disc. (**?**). Explains also why no large outburst (ie a low contrast between the brightest and dimmest X-ray emission) in Cygnus X-1 (x3) (Grinberg et al. 2014) : without an outer cool disc, the thermal instability resulting from the ionization of Hydrogen cannot occur (REF?). No quiescent state in Cyg X-1 : it is an argument in favor of the existence of a cool disc in the hard state.

3.3. Mass and angular momentum accretion rates

If halted mass accretion, might be due to radiative heating from the X-ray source (Sugimura et al. 2018) : if circularization radius > 0.04 times the Bondi radius (for us, the accretion radius?), much lower accretion rate than Bondi (for us, BHL?). But their work depends also on isotropic or anisotropic X-ray source, alpha viscosity parameter, etc...

4. Observational consequences

4.1. Disc mass and morphology

5. Conclusion

In this paper, we connected the orbital scale, at which the wind unfolds, to the one of the accretion radius, at which the flow is significantly beamed by the gravitational field of the compact object and where HD shocks form, all the way down to the outer edge of the NS magnetosphere.

currently, lack of conclusive evidence in favor of the presence of a permanent disc in SgXB (Bozzo et al. 2008; Shakura et al. 2012; Romano et al. 2015; Hu et al. 2017) : is it because it is could be truncated by the magnetosphere and not hot enough to contribute significantly compared to the accretion columns at the NS poles?

What about the impact of other orbital scale structures on the formation of wind capture disc? Impact of corotating (i.e. at the stellar rotation rate) interaction region (spiral-shaped density and velocity enhancements due to irregularities on the stellar surface such as local luminosity increase by 10%). Observed in single OB stars. In low luminosity SgXB and SFXT, proposed by Bozzo et al. (2017) as a possible origin of the super-orbital modulation (between stellar and orbital period) observed, as the accretor crosses the CIR. Rq : since the super orbital period is usually of the order of a few times the orbital period only, it means that the stellar rotation period and the orbital period must be quite different (while I expected stars to be in synchronous rotation in HMXB...)

which connect the different scales

significant deviation from

bridge the gap between the / starts to resemble RLOF

The interest is twofold (Martínez-Núñez et al. 2017)

What about the micro-structure? Clumps small compared to accretion radius for such small wind speed.

Acknowledgements. Hugues Sana for his insights on binary evolution Antonios Manousakis for fruitful discussions about the underlying computational aspects IEM has received funding from the Research Foundation Flanders (FWO) and the European Union's Horizon 2020 research and innovation program under the Marie Skłodowska-Curie grant agreement No 665501. IEM and JOS are grateful for the hospitality of the International Space Science Institute (ISSI), Bern, Switzerland which sponsored a team meeting initiating a tighter collaboration between massive stars wind and X-ray binaries communities. IEM also thanks Peter Kretschmar, Victoria Grinberg and Felix Fürst for the fruitful discussions and the relevant comments they made on the present work. The simulations were conducted on the Tier-1 VSC (Flemish Supercomputer Center funded by Hercules foundation and Flemish government).

References

Abbott, B. P., Abbott, R., Abbott, T. D. and Al, E. (2016), 'GW151226: Observation of Gravitational Waves from a 22-Solar-Mass Binary Black Hole Coalescence', *Phys. Rev. Lett.* **116**(24), 241103.
URL: *http://link.aps.org/doi/10.1103/PhysRevLett.116.241103*

Bozzo, E., Falanga, M. and Stella, L. (2008), 'Are There Magnetars in High-Mass X-Ray Binaries? The Case of Supergiant Fast X-Ray Transients', *Astrophys. J.* **683**(2), 1031–1044.
URL: *http://iopscience.iop.org/article/10.1086/589990*

Bozzo, E., Oskinova, L., Lobel, A. and Hamann, W. R. (2017), 'On the super-orbital modulation of supergiant high mass X-ray binaries', *Astron. Astrophys. Vol. 606, id.L10, 4 pp.* **10**, 4–7.
URL: *http://arxiv.org/abs/1710.01877 http://dx.doi.org/10.1051/0004-6361/201731930*

Castor, J. I., Abbott, D. C. and Klein, R. I. (1975), 'Radiation-driven winds in Of stars', *Astrophys. J.* **195**, 157.
URL: *http://adsabs.harvard.edu/abs/1975ApJ...195..157C*

Duchêne, G. and Kraus, A. (2013), 'Stellar Multiplicity', *Annu. Rev. Astron. Astrophys.* **51**(1), 269–310.
URL: *http://arxiv.org/abs/1303.3028 http://adsabs.harvard.edu/abs/2013ARA%26A..51..2*

Edgar, R. G. (2004), 'A review of Bondi–Hoyle–Lyttleton accretion', *New Astron. Rev.* **48**(10), 843–859.
URL: *http://linkinghub.elsevier.com/retrieve/pii/S1387647304000739*

Forman, W., Jones, C., Tananbaum, H., Gursky, H., Kellogg, E. and Giacconi, R. (1973), 'UHURU Observations of the Binary X-Ray Source 2u 0900-40', *Astrophys. J.* **182**, L103.
URL: *http://adsabs.harvard.edu/doi/10.1086/181229*

Fürst, F., Pottschmidt, K., Wilms, J., Tomsick, J. A., Bachetti, M., Boggs, S. E., Christensen, F. E., Craig, W. W., Grefenstette, B. W., Hailey, C. J., Harrison, F., Madsen, K. K., Miller, J. M., Stern, D., Walton, D. J. and Zhang, W. (2014), 'NuSTAR discovery of a luminosity dependent cyclotron line energy in Vela X-1', *Astrophys. J.* **780**(2).
URL: *http://arxiv.org/abs/1311.5514 http://dx.doi.org/10.1088/0004-637X/780/2/133*

Gimenez-Garcia, A., Shenar, T., Torrejon, J. M., Oskinova, L., Martinez-Nunez, S., Hamann, W.-R., Rodes-Roca, J. J., Gonzalez-Galan, A., Alonso-Santiago, J., Gonzalez-Fernandez, C., Bernabeu, G. and Sander, A. (2016), 'Measuring the stellar wind parameters in IGR J17544-2619 and Vela X-1 constrains the accretion physics in Supergiant Fast X-ray Transient and classical Supergiant X-ray Binaries', *Astron. Astrophys.* **591**(A26), 25.
URL: *http://arxiv.org/abs/1603.00925 http://dx.doi.org/10.1051/0004-6361/201527551 http://adsabs.harvard.edu/abs/2016arXiv160300925G*

Gräfener, G., Koesterke, L. and Hamann, W.-R. (2002), 'Line-blanketed model atmospheres for WR stars', *Astron. Astrophys.* **387**(1), 244–257.
URL: *http://www.aanda.org/10.1051/0004-6361:20020269*

Grinberg, V., Hell, N., El Mellah, I., Neilsen, J., Sander, A. A. C., Leutenegger, M., Fürst, F., Huenemoerder, D. P., Kretschmar, P., Kühnel, M., Martínez-Núñez, S., Niu, S., Pottschmidt, K., Schulz, N. S., Wilms, J. and Nowak, M. A. (2017), 'The clumpy absorber in the high-mass X-ray binary Vela X-1', *Astron. Astrophys. Vol. 608, id.A143, 18 pp.* **608**.
URL: *http://arxiv.org/abs/1711.06743 http://dx.doi.org/10.1051/0004-6361/201731843*

Grinberg, V., Pottschmidt, K., Böck, M., Schmid, C., Nowak, M. A., Uttley, P., Tomsick, J. A., Rodriguez, J., Hell, N., Markowitz, A., Bodaghee, A., Bel, M. C., Rothschild, R. E. and Wilms, J. (2014), 'Long term variability of Cygnus X-1: VI. Energy-resolved X-ray variability 1999-2011', *arXiv.org* .
URL: *http://arxiv.org/abs/1402.4485%0Ahttp://dx.doi.org/10.1051/0004-6361/201322969*

Hamann, W.-R. and Koesterke, L. (1998), 'Spectrum formation in clumped stellar winds: consequences for the analyses of Wolf-Rayet spectra', *Astron. Astrophys* **335**, 1003–1008.
URL: *http://articles.adsabs.harvard.edu/cgi-bin/nph-iarticle_query?1998A%26A...335.1003H&data_type=PDF_HIGH&whole_paper=YES&*

Hiltner, W. A., Werner, J. and Osmer, P. (1972), 'Binary Nature of the B Supergiant in the Error Box of the VELA X-Ray Source', *Astrophys. J.* **175**, L19.
URL: *http://adsabs.harvard.edu/doi/10.1086/180976*

Horedt, G. P. (2000), 'Pressure Effects in Line Accretion', *Astrophys. J.* **541**(2), 821–830.
URL: *http://iopscience.iop.org/0004-637X/541/2/821/fulltext/*

Hu, C.-P., Chou, Y., Ng, C. Y., Lin, L. C.-C. and Yen, D. C.-C. (2017), 'Evolution of Spin, Orbital, and Superorbital Modulations of 4U 0114+650', *Astrophys. Journal, Vol. 844, Issue 1, Artic. id. 16, 10 pp. (2017).* **844**.
URL: *http://arxiv.org/abs/1706.03902 http://dx.doi.org/10.3847/1538-4357/aa79a3 http://arxiv.org/abs/1706.03902%0Ahttp://dx.doi.org/10.3847/1538-4357/aa79a3*

Illarionov, A. F. and Sunyaev, R. A. (1975), 'Why the Number of Galactic X-ray Stars Is so Small?', *Astron. Astrophys.* **39**.
URL: *http://adsabs.harvard.edu/abs/1975A%26A....39..185I*

Lucy, L. B. and Solomon, P. M. (1970), 'Mass Loss by Hot Stars', *Astrophys. J.* **159**, 879.
URL: *http://adsabs.harvard.edu/abs/1970ApJ...159..879L*

Manousakis, a., Walter, R. and Blondin, J. (2013), 'Accretion in supergiant High Mass X-ray Binaries'.
URL: *http://arxiv.org/abs/1310.8205v1*

Martínez-Núñez, S., Kretschmar, P., Bozzo, E., Oskinova, L. M., Puls, J., Sidoli, L., Sundqvist, J. O., Blay, P., Falanga, M., Fürst, F., Gímenez-García, A., Kreykenbohm, I., Kühnel, M., Sander, A., Torrejón, J. M. and Wilms, J. (2017), 'Towards a Unified View of Inhomogeneous Stellar Winds in Isolated Supergiant Stars and Supergiant High Mass X-Ray Binaries', *Space Sci. Rev.* **212**(1-2), 59–150.
URL: *http://arxiv.org/abs/1701.08618 http://dx.doi.org/10.1007/s11214-017-0340-1*

Quaintrell, H., Norton, A. J., Ash, T. D. C., Roche, P., Willems, B., Bedding, T. R., Baldry, I. K. and Fender, R. P. (2003), 'The mass of the neutron star in Vela X-1 and tidally induced non-radial oscillations in GP Vel', *Astron. Astrophys.* **401**(1), 313–323.
URL: *http://adsabs.harvard.edu/abs/2003A&A...401..313Q http://arxiv.org/abs/astro-ph/0301243 http://dx.doi.org/10.1051/0004-6361:20030120*

Rawls, M. L., Orosz, J. A., McClintock, J. E., Torres, M. A. P., Bailyn, C. D. and Buxton, M. M. (2011), 'Refined Neutron-Star Mass Determinations for Six Eclipsing X-Ray Pulsar Binaries', *Astrophys. Journal, Vol. 730, Issue 1, Artic. id. 25, 11 pp. (2011).* **730**.
URL: *http://arxiv.org/abs/1101.2465 http://dx.doi.org/10.1088/0004-637X/730/1/25*

Romano, P., Bozzo, E., Mangano, V., Esposito, P., Israel, G., Tiengo, A., Campana, S., Ducci, L., Ferrigno, C. and Kennea, J. A. (2015), 'Giant outburst from the supergiant fast X-ray transient IGR J17544-2619: accretion from a transient disc?', *Astron. Astrophys.* **576**, 5–9.
URL: *http://arxiv.org/abs/1502.04717 http://dx.doi.org/10.1051/0004-6361/201525749*

Sander, A. A. C., Fürst, F., Kretschmar, P., Oskinova, L. M., Todt, H., Hainich, R., Shenar, T. and Hamann, W.-R. (2017), 'Coupling hydrodynamics with comoving frame radiative transfer: II. Stellar wind stratification in the high-mass X-ray binary Vela X-1', *eprint arXiv:1708.02947* .
URL: *http://arxiv.org/abs/1708.02947*

Sander, A. A. C., Hamann, W.-R., Todt, H., Hainich, R. and Shenar, T. (2017), 'Coupling hydrodynamics with comoving frame radiative transfer. I. A unified approach for OB and WR stars', *Astron. Astrophys. Vol. 603, id.A86, 14 pp.* **603**.
URL: *http://adsabs.harvard.edu/abs/2017A%26A...603A..86S*

Schure, K. M., Kosenko, D., Kaastra, J. S., Keppens, R. and Vink, J. (2009), 'A new radiative cooling curve based on an up to date plasma emission code', *Astron. Astrophys. Vol. 508, Issue 2, 2009, pp.751-757* **757**, 751–757.
URL: *http://arxiv.org/abs/0909.5204%0Ahttp://dx.doi.org/10.1051/0004-6361/200912495 http://arxiv.org/abs/0909.5204 http://dx.doi.org/10.1051/0004-6361/200912495*

Shakura, N., Postnov, K., Kochetkova, A. and Hjalmarsdotter, L. (2012), 'Theory of quasi-spherical accretion in X-ray pulsars', *Mon. Not. R. Astron. Soc.* **420**(1), 216–236.
URL: *http://arxiv.org/abs/1110.3701 http://dx.doi.org/10.1111/j.1365-2966.2011.20026.x*

Sugimura, K., Hosokawa, T., Yajima, H., Inayoshi, K. and Omukai, K. (2018), 'Stunted accretion growth of black holes by combined effect of the flow angular momentum and radiation feedback', *Mon. Not. R. Astron. Soc* **000**(0000), 0–0.
URL: *https://arxiv.org/pdf/1802.07264.pdf*

Vink, J. S., de Koter, A. and Lamers, H. J. G. L. M. (2001), 'Mass-loss predictions for O and B stars as a function of metallicity', *Astron. Astrophys. v.369, p.574-588* **369**, 61–64.
URL: *http://arxiv.org/abs/astro-ph/0101509 http://dx.doi.org/10.1051/0004-6361:20010127 http://arxiv.org/abs/astro-ph/0101509%0Ahttp://dx.doi.org/10.1051/0004-6361:20010127*

Xia, C., Teunissen, J., Mellah, I. E., Chané, E. and Keppens, R. (2018), 'MPI-AMRVAC 2.0 for Solar and Astrophysical Applications', *Astrophys. J. Suppl. Ser.* **234**(2), 30.
URL: *http://stacks.iop.org/0067-0049/234/i=2/a=30?key=crossref.eaf55349f020bd924d414adc8d989a32*